Wing (Ib) cells in frog taste discs detect dietary unsaturated fatty acids

Yukio Okada[1,*], Toshihiro Miyazaki[2], Rie Fujiyama[1], and Kazuo Toda[1]

[1]*Integrative Sensory Physiology* and [2]*Cell Biology, Graduate School of Biomedical Sciences, Nagasaki University, Nagasaki, Nagasaki 852-8588, Japan*

*Corresponding author: Integrative Sensory Physiology, Graduate School of Biomedical Sciences, Nagasaki University, 1-7-1 Sakamoto, Nagasaki, Nagasaki 852-8588, Japan.
Tel: +81-95-819-7637; Fax: +81-95-819-7639.
E-mail: okada@nagasaki-u.ac.jp (Y. Okada).

Abstract

The effects of unsaturated fatty acids on membrane properties were studied using conventional whole-cell patch-clamp recording of isolated wing (Ib) cells in frog taste discs. Applying arachidonic acid to the bath induced monophasic inward currents in 60% of wing cells and biphasic inward and outward currents in the other cells. Intracellular dialysis of arachidonic acid did not induce an inward current; however, it enhanced a slowly developing Ba^{2+}-sensitive outward current. The effects of various unsaturated fatty acids were explored under the condition of Cs^{+} internal solution. Linoleic and α-linolenic acids induced large inward currents. Oleic, eicosapentaenoic, and docosahexaenoic acids elicited the same inward currents as those of arachidonic acid. Wing cells, under the basal condition with Cs^{+} internal solution, displayed a small inward current of -1.1 ± 0.1 pA/pF at -50 mV (n=40), in which the peak existed at a membrane potential of -49 mV. Removing external Ca^{2+} further increased the inward current by -2.9 ± 0.3 pA/pF at -50 mV (n=4) from the basal current and the peak was located at -55 mV. External linoleic acid (50 μM) also induced a similar inward current of -5.6 ± 0.6 pA/pF at -50 mV (n=19) from the basal current and the peak was located at -61 mV. External Ca^{2+}-free saline and linoleic acid induced similar current/voltage (*I/V*) relationships elicited by a ramp voltage as well as voltage steps. Linoleic acid-induced currents were not influenced by replacing internal EGTA with BAPTA, whereas inward currents disappeared under the elimination of external Na^{+} and addition of flufenamic acid. These results suggest that dietary unsaturated fatty acids may depolarize wing (Ib) cells, which affects the excitability of these cells.

1. Introduction

Fats in foods are not only essential nutrients, but also enhance deliciousness in taste. Secreted lipases in the oral cavity of mammals digest dietary triacylglycerides, resulting in the production of free fatty acids (Kawai and Fushiki, 2003). Free fatty acids can stimulate taste cells. In rat taste cells, free fatty acids such as arachidonic acid were shown to inhibit delayed rectifying K^+ channels, while lipids enhanced inward rectifying K^+ channels (Gilbertson et al., 1997). Arachidonic acid also enters cells and is rapidly metabolized to oxygenated products by several distinct enzymes, including cyclooxygenases, lipoxygenases, or epoxygenases (cytochrome P450s) (Needleman et al., 1986). These products contribute to a number of physiological processes as autacoids.

Several different fatty acid-binding proteins that may initiate fatty acid taste transduction have recently been identified, including Src TK (Src family tyrosine kinase)-activating CD36 (Fukuwatari et al., 1997; Laugerette et al., 2005) and G-protein-coupled receptors (GPR40 and GPR120) (Matsumura et al., 2009; Cartoni et al., 2010; Galindo et al., 2012). Linoleic acid, which is a typical unsaturated fatty acid, activates TRPM5 ion channels, resulting in the depolarization of mouse taste cells (Liu et al., 2011).

Frogs eat moving prey and prefer elongated insects such as crickets that move across their visual field. Habitat differences have been reported in prey nutritional composition. In cold climates, animals are more likely to have higher levels of unsaturated fatty acids to retain metabolism and flexibility. Lipids are important in amphibian diets, both in their quantity and quality (Browne, 2009). The amount and types of lipids must be optimal. The amounts and types of saturated and unsaturated

fatty acids in particular must be balanced. Insects contain lipids in the range between 10% and 30% of their fresh weight basis, and have relatively high levels of essential C18 fatty acids, oleic acid (18:1), linoleic acid (18:2), and linolenic acid (18:3) (DeFoliart, 1991; Ogg et al., 1993). Similarly, freshwater fishes contain high concentrations of oleic and linoleic acids (Li et al., 2011).

Fatty acids absorbed from the small intestine are considered to affect health in humans and animals. Omega-3 fatty acids (α-linolenic acid, eicosapentaenoic acid, and docosahexaenoic acid) were shown to stimulate GPR120 in adipose tissue, promoting anti-inflammatory effects (Oh et al., 2010). These fatty acids have also been reported to lower blood pressure in humans. Omega-3 fatty acids were recently confirmed to lower blood pressure by directly activating Ca^{2+}-dependent K^+ channels (Hoshi et al., 2013).

In the present study, we showed that C18 fatty acids such as linoleic acid elicited a novel inward current in the wing (Ib) cells of frog taste discs.

2. Materials and methods

2.1. Cell preparation

Adult bullfrogs (*Rana catesbeiana*) weighing 250-550 g were used for the experiment over the course of a year. Experiments were performed in accordance with the Guidelines for Animal Experimentation of Nagasaki University with approval of the Institutional Animal Care and Use Committee. The keeping of bullfrogs (invasive alien species) was approved by the Ministry of the Environment of Japan (approval number 06000204). Taste disc cells were isolated from the tongue of decapitated and pithed animals, as described previously (Okada et al., 2001). Fungiform papillae were dissected from the tongue in nominal Ca^{2+}-free saline and stored in Ca^{2+}-free saline

containing 2 mM EDTA (ethylenediaminetetraacetic acid) for 10 min. These papillae were bathed in the same saline containing 10 mM L-cysteine and 10 U/ml papain (Sigma, St Lois, MO, USA) for 10-13 min. The papillae were then rinsed with normal saline, and individual cells were dissociated by gentle trituration in normal saline. Isolated taste disc cells showing a characteristic morphology were readily distinguished from the other cells and classified into rod and wing cells (Okada et al., 1996; Bigiani et al., 1998). Rod cells had one dendrite-like process while wing cells had two or three dendrite-like processes connected to each other by a sheet-like structure.

2.2. Electrophysiological recording

Voltage-clamp recording was performed in the whole-cell configuration (Hamil et al., 1981) using a CEZ 2300 patch-clamp amplifier (Nihon Kohden, Tokyo, Japan) or an EPC-7 plus amplifier (HEKA Elektronik, Lambrecht, Germany). Patch pipettes were pulled from Pyrex glass capillaries containing a fine filament (Summit Medical, Tokyo, Japan and Ken Enterprise, Kanagawa, Japan) with a two-stage puller (Narishige PD-5, Tokyo, Japan). The tips of the electrodes were heat-polished with a microforge (Narishige MF-80). The resistance of the resulting patch electrode was 5-10 MΩ when filled with internal solution. The formation of 5-20 GΩ seals between the patch pipette and cell surface was facilitated by applying weak suction to the interior of the pipette. The patch membrane was broken by applying strong suction, resulting in a sudden increase in capacitance. Recordings were made from taste disc cells that had been allowed to settle on the bottom of a chamber placed on the stage of an inverted microscope (Olympus IMT-2, Tokyo, Japan). The recording pipette was positioned with a hydraulic micromanipulator (Narishige WR-88). The current signal was low-pass-filtered at 5 kHz, digitized at 125 kHz using a TL-1 interface (Axon

Instruments, Union City, CA, USA), acquired at a sampling rate of 0.25-5 kHz using a computer running the pCLAMP 5.5 software (Axon Instruments), and stored on a hard disk. pCLAMP was also used to control the digital-analogue converter for the generation of the clamp protocol. The indifferent electrode was a chloriding silver wire. Voltages were corrected for the liquid junction potential between the external solution and internal solution. Capacitance and series resistance were compensated for, as appropriate. In voltage ramp-mode experiments, the voltage was held at -50 mV, which was close to the resting potential. The value of -50 mV was compensated to -54 mV when K^+ internal solution was used and -55 mV when Cs^+ internal solution was used for the correction of the liquid junction potential. The whole-cell current-voltage (*I/V*) relationship was obtained from the current generated by the 167 mV/s voltage ramp from -100 to +100 mV. In some cases, current-voltage relationships were obtained from the currents generated by 400 ms voltage-step pulses between -105 and +95 mV in 20 mV increments from a holding potential of -85 mV. The voltage in step pulses also compensated for the liquid junction potential. Data were analyzed with pCLAMP and Origin 8.1 and 8.5 (Origin Lab, Northampton, MA, USA). Fatty acid-induced currents were estimated as the difference between response and basal currents. Unless stated otherwise, the data are presented as means ± S.E.M., with significance being tested by the Student's t test. Differences were considered significant if $P < 0.05$.

2.3. Solutions and drugs

Normal saline solution consisted of (in mM): NaCl, 115; KCl, 2.5; $CaCl_2$, 1.8; Hepes (4-(2-hydroxyethyl)-1-piperazineethanesulfonic acid), 10; glucose, 20; pH 7.2. The pH of normal saline and other solutions was adjusted by Tris

(tris(hydroxymethyl)aminomethane) base. External Na^+-free solution was prepared by replacing Na^+ and K^+ with $NMDG^+$ (N-methyl-D-glucamine$^+$). External Ca^{2+}-free solution contained 1 mM EGTA (ethylene glycol-bis-(β-aminoethyl ether)-N,N,N',N'-tetraacetic acid). Solution exchange was performed by gravity flow. Arachidonic acid (50 mM, Sigma and Cayman, Ann Arbor, MI, USA), linoleic acid (50 mM, Cayman), α-linolenic acid (50 mM, Cayman), docosahexaenoic acid (50 mM, Cayman), eicosapentaenoic acid (50 mM, Cayman), oleic acid (50 mM, Cayman), stearic acid (50 mM, Sigma), eicosatetraynoic acid (ETYA, 50 mM, Sigma) were dissolved in dimethylsulphoxide (DMSO) for the stock solution. Samples of the stock solution were added to the external solution or internal solution to give the desired final solution. Flufenamic acid (100 μM, Sigma) and carbenoxolone (CBX, 50-100 μM, Sigma) were directly dissolved in normal saline solution. Standard K^+ internal solution contained (in mM): KCl, 100; $CaCl_2$, 0.1; $MgCl_2$, 2; EGTA, 1; Hepes, 10; pH 7.2. In some experiments, internal K^+ was replaced with Cs^+. BAPTA (1,2-bis(o-aminophenoxy)ethane-N,N,N',N'-tetraacetic acid, 10 mM, Sigma) was dissolved in internal solution.

All experiments were carried out at room temperature (20-25°C).

3. Results

3.1. Basal electrical properties of wing (Ib) cells

The basal properties of wing (Ib) cells in frog taste discs were previously reported (Okada et al., 2001). Briefly, under standard K^+ internal solution, frog wing cells displayed a resting potential of -46.7 ± 1.9 mV (n=20), input resistance of 4.6 ± 0.4 GΩ (n=20), and membrane capacitance of 13.6 ± 0.4 pF (n=20). As previously reported

(Miyamoto et al., 1991), almost all wing cells displayed transient TTX-sensitive Na^+ currents followed by sustained Ba^{2+}-sensitive K^+ currents in response to depolarizing voltage steps from a holding potential of -84 mV. The current-voltage relationships obtained by a voltage ramp were bell-shaped in the wing cells (e.g. see Fig. 1Ba, Da).

3.2. Arachidonic acid-induced currents in K^+ internal solution

When 10 μM arachidonic acid was added to the external solution, the wing cells displayed the appearance of a small inward current of -1.5 ± 0.2 pA/pF from a basal current of -0.2 ± 0.1 pA/pF at -50 mV, n=4) at the negative membrane potential and a decrease in the outward current (from 8.1 ± 1.6 pA/pF at +50 mV to 6.8 ± 0.8 pA/pF at +50 mV, $P > 0.05$, n=4) at the positive membrane potential. After washout, the current level returned to -0.2 ± 0.1 pA/pF at -50 mV and 10.7 ± 3.2 pA/pF at +50 mV (n=4). The higher concentration of arachidonic acid (50 μM) induced a marked increase in the inward current (Fig. 1) at the negative membrane potential. The peak of the arachidonic acid-induced current (-3.2 ± 0.4 pA/pF at -50 mV from the basal current of -0.4 ± 0.2 pA/pF at -50 mV, n=10) was observed in the membrane potential between -50 and -60 mV. Six of 10 wing cells displayed inward currents only (Fig. 1A, B), while the other four cells showed the reverse from an inward to outward current at -50 mV (Fig. 1C, D). The rod cells displayed an initial decrease and transient increase in the outward current and the final appearance of the inward current at -50 mV in response to external 50 μM arachidonic acid (n=4). This complicated property in the rod cells was not analyzed further.

We considered that the late outward component of the biphasic type may be due to the effect of internal arachidonic acid entering through the membrane. When arachidonic acid (50 μM) was dialyzed into the wing cells, it induced a slowly

186 developing outward current (Fig. 2A). The outward current at +50 mV increased from
187 5.1 ± 1.6 pA/pF to 18.7 ± 2.0 pA/pF ($P < 0.05$, n=3) and was markedly inhibited by
188 external 5 mM Ba^{2+} (Fig. 2B). Internal arachidonic acid never elicited an inward current
189 in the wing cells. Internal 50 μM ETYA (a non-metabolizable analog of arachidonic
190 acid) also enhanced the outward current (Fig. 2C), while internal linoleic acid had no
191 effect (Fig. 2D).
192 3.3. Unsaturated fatty acid-induced currents in Cs^+ internal solution
193 The effects of various fatty acids were explored under the condition in which
194 outward K^+ currents were eliminated by replacing internal K^+ with Cs^+ (Fig. 3A, B).
195 Saturated stearic acid (30 μM) induced almost no current. Linoleic acid and α-linolenic
196 acid induced relatively large inward currents (Fig. 3C). Oleic acid, eicosapentaenoic
197 acid, and docosahexaenoic acid elicited the same inward currents as those of
198 arachidonic acid.
199 Under the basal condition, wing (Ib) cells displayed a novel inward current (-1.1 ±
200 0.1 pA/pF at -50 mV, n=40) in Cs^+ internal solution (Fig. 4A). The peak of the inward
201 current was located at -49 mV (Fig. 4A). The half-maximum voltage ($V_{1/2}$) for
202 activation was -74 mV (Fig. 4B). This was observed in 32 of 40 cells. The shape of the
203 fatty acid-induced inward current was similar to that of connexin hemichannels in the
204 external Ca^{2+}-free condition (Verselis and Srinivas, 2008). Removing external Ca^{2+} also
205 induced an inward current of -2.9 ± 0.3 pA/pF at -50 mV (n=4) from a basal current of
206 -1.1 ± 0.1 pA/pF at -50 mV (n=4) (Fig. 4C). The peak of the inward current was located
207 at -55 mV (Fig. 4C) and $V_{1/2}$ was -69 mV (Fig. 4D). External linoleic acid (50 μM)
208 elicited an inward current of -5.6 ± 0.6 pA/pF at -50 mV (n=19) from a basal current of
209 -1.2 ± 0.1 pA/pF at -50 mV (n=19) in Cs^+ internal solution. The peak of the inward

current was located at -61 mV (Fig. 4E) and the $V_{1/2}$ was -77 mV (Fig. 4F). The linoleic acid-induced inward current reversed at a membrane potential of +0.7 ± 0.5 mV (n=19).

The biophysical properties of external Ca^{2+}-free- and linoleic acid-induced currents were analyzed by voltage steps between -105 mV and +95 mV for 400 ms from a holding potential of -85 mV. Wing (Ib) cells displayed transient inward currents (TTX-sensitive, voltage-gated Na^+ currents) and then small sustained currents in response to depolarizing steps in normal saline solution (Fig. 5A, B). When external Ca^{2+} was removed, almost instantaneous and sustained current appeared in response to the depolarizing steps (n=3) (Fig. 5B). *I-V* relationships by voltage steps were similar to those by the ramp voltage (Fig. 5C). Linoleic acid-induced current also displayed similar characteristics in *I-V* relationships by voltage steps (Fig. 5E, F). During Ca^{2+}-free-induced and linoleic acid-induced responses, the voltage step to -105 mV from a holding potential of -85 mV induced an apparent sustained outward current, which was actually a decrease in the sustained inward current (Fig. 5C, F). The voltage-gated Na^+ current at -25 mV from a holding potential of -85 mV decreased from -63.9 ± 5.8 pA/pF to -22.8 ± 8.6 pA/pF ($P < 0.05$, n=4) in response to external Ca^{2+}-free saline solution (Fig. 5A, B). Linoleic acid (50 μM) also decreased the Na^+ current from -51.4 ± 6.5 pA/pF to -14.7 ± 6.3 pA/pF ($P < 0.05$, n=3) (Fig. 5D, E).

Linoleic acid also elicited an inward current of -5.6 ± 1.1 pA/pF at -50 mV (n=3) from a basal current of -0.3 ± 0.1 pA/pF at -50 mV (n=3) under the condition in which internal 1 mM EGTA was replaced with 10 mM BAPTA, which suggested that the change in internal Ca^{2+} concentrations may not be concerned with inward currents. On the other hand, linoleic acid-induced inward currents disappeared under the condition in which external Na^+ was replaced with $NMDG^+$ (n=5) (Fig. 6A, B). Flufenamic acid (a

non-selective blocker of cationic channels, 100 μM) markedly inhibited inward currents (n=3) (Fig. 6C, D).

Flufenamic acid was shown to markedly inhibit connexin hemichannels, whereas carbenoxolone inhibited pannexin hemichannels (Bruzzone et al., 2005). Interestingly, carbenoxolone (50 μM) also elicited an inward current of -3.3 ± 0.5 pA/pF at -50 mV (n=6) from a basal current of -1.0 ± 0.1 pA/pF at -50 mV (n=6).

4. Discussion

The present results showed that wing (Ib) cells in frog taste discs could respond to various unsaturated fatty acids, resulting in conductance increase. Fatty acids induced two different effects; activation of an inward current from the outside of the cell membrane and activation of an outward current from the inside.

4.1. Comparison of the responses to unsaturated fatty acids with other cell types

Arachidonic acid, a typical polyunsaturated fatty acid, has various actions on living cells (Meves, 2008). In most cells, it inhibits outward K^+ currents. In the present study, external 10 μM arachidonic acid inhibited outward currents at +50 mV by 15%. Higher concentrations of this fatty acid may more markedly inhibit the outward current; however, inhibition was blurred by the subsequent activation of another conductance. Alternatively, intracellular perfusion of arachidonic acid from the patch pipette enhanced the outward K^+ current only in wing (Ib) cells. This effect was specific to arachidonic acid, although linoleic acid also had a similar effect on the mammalian two pore domain K^+ channel (Fink et al., 1998). The enhancing effect on the outward current cannot be due to its metabolite, since ETYA (a non-metabolizable analog of arachidonic acid and inhibitor of its metabolism) also enhanced the outward current.

Transient receptor potential (TRP) channels play various important roles in many cell types. Polyunsaturated fatty acids such as linoleic acid activate light sensitive TRP channels in *Drosophila* photoreceptors (Chyb et al., 1999). The lipoxygenase metabolites of arachidonic acid were shown to activate capsaicin-sensitive TRPV1 channels (Hwang et al., 2000) and the epoxygenase metabolites of the fatty acid activated mechano-sensitive TRPV4 channels (Watanabe et al., 2003). Polyunsaturated acids and their metabolites may act as second messengers in these channels.

Unsaturated fatty acids elicited a cationic inward current only from the outside of the cell membrane in frog wing (Ib) cells. Although these fatty acids may not act through an intracellular metabolic pathway, these hydrophobic substances act as extracellular ligands for the activation of cationic conductance. External linoleic acid (50 μM) did not elicit the glossopharyngeal neural response in frogs (Y. Okada, unpublished data), which suggested that wing (Ib) cells may act as glial-like cells (not taste cells). Linoleic acid at 20-30 μM was shown to activate cationic conductance in the taste cells of mammals (Liu et al., 2011; Dramane et al., 2012), while thousand-fold concentrations of fatty acids are needed to elicit neural responses (Cartoni et al., 2010).

4.2. The possible role of unsaturated fatty acid-induced currents in wing (Ib) cells

Frogs ingest insects almost intact, which indicates that soft tissues beneath the chitin exoskeleton cannot release free fatty acids into the oral cavity. Freshwater in the river contain about 200 nM oleic acid (Fatoki and Vernon, 1989), while the total concentration of free fatty acids in the river freshwater may be under one μM. It is unclear whether frogs can detect free fatty acids lower than one μM. Fatty acids are absorbed from the small intestine, and those containing more than 10-12 carbon atoms are transported in the blood vessels as they bind with albumin. Unsaturated fatty acids

282 are classified into omega-3 and omega-6 fatty acids. Omega-3 fatty acids such as
283 docosahexaenoic acid bind to GPR120 in adipose tissue and promote anti-inflammatory
284 effects (Oh et al., 2010). They also lower blood pressure by directly activating
285 Ca^{2+}-dependent K^+ channels without Ca^{2+} increase (Hoshi et al., 2013). Cell membranes
286 composed of phospholipids display membrane fluidity. Fatty acids with many
287 double-bonds markedly affect this fluidity. The efficiency of docosahexaenoic acid
288 (C22:6) on aortic K^+ channels was shown to be larger than that of linoleic acid (C18:2).
289 The efficiency for the inward current in the wing cells was shown to be the opposite;
290 linoleic acid may induce an inward current by affecting the protein-lipid membrane
291 interface (Schmidt et al., 2006).
292 Fatty acid-induced currents in the wing cells also displayed voltage-dependency.
293 Connexin hemichannels have intrinsic voltage-dependent gating (Verselis and Strinivas,
294 2008) and are activated by linoleic acid (Figueroa et al., 2013). In mammals, gustatory
295 stimuli was suggested to cause taste cells to release ATP through pannexin
296 hemichannels (Huang et al., 2007); however, an electrophysiological study indicated the
297 significant role of connexin rather than pannexin (Romanov et al., 2007). Finally,
298 CALHM1 (calcium homeostasis modulator 1) ion channels have been identified as a
299 voltage-gated ATP release channel required for taste perception (Taruno et al., 2013).
300 CALHM1 shares functional and structural similarities with connexin (Siebert et al.,
301 2013). These channels enable the permeation of large charged molecules. Wing cells
302 also may release large charged molecules without exocytosis.
303 Mammalian taste cells release ATP at a voltage more than 0 mV, which indicates the
304 important role of voltage-gated Na^+ channels for large depolarization (Romanov et al.,
305 2007). On the other hand, fatty acid-induced currents in the wing cells were strongly

306 activated at the voltage of the resting membrane potential (about -50 mV). This property
307 may have the advantage of maintaining the membrane potential in the vicinity of -50
308 mV. Voltage-gated Na^+ channels may almost be inactivated at -50 mV. Fatty
309 acid-induced conductance may protect wing cells from exciting or causing excessive
310 hyperpolarization.
311 In conclusion, dietary fatty acids may directly activate a hemichannel-like
312 conductance in wing (Ib) cells, which depolarizes the cells. The depolarization of wing
313 (Ib) cells may affect their excitability.
314
315 **Acknowledgments**
316 This work was supported by Grants-in-Aid (20570073) from Japan Society for the
317 Promotion of Science (to Y.O.).
318

References

Bigiani, A., Sbarbati, A., Osculati, F., Pietra, P., 1998. Electrophysiological characterization of a putative supporting cell isolated from the frog taste disk. J. Neurosci. 18, 5136-5150

Browne, R.K., 2009. Amphibian diet and nutrition. Amphibian Ark Science and Research, Apple Valley, MN, USA. (http://aark.portal.isis.org/ResearchGuide/Amphibian%20husbandry/Amphibian%20diet%20and%20nutrition.pdf)

Bruzzone, R., Barbe, M.T., Jakob, N.J., Monyer, H., 2005. Pharmacological properties of homomeric and heteromeric pannexin hemichannels expressed in Xenopus oocytes. J. Neurochem. 92. 1033-1043.

Cartoni, C., Yasumatsu, K., Ohkuri, T., Shigemura, N., Yoshida, R., Godinot, N., le Coutre, J., Ninomiya, Y., Damak, S., 2010. Taste preference for fatty acids is mediated by GPR40 and GPR120. J. Neurosci. 30, 8376-8382.

Chyb, S., Raghu, P., Hardie, R.C., 1999. Polyunsaturated fatty acids activate the Drosophila light-sensitive channels TRP and TRPL. Nature 397, 255-259.

DeFoliart, G.R., 1991. Insect fatty acids: similar to those of poultry and fish in their degree of unsaturation, but higher in the polyunsaturates. Food Insects Newsl. 4, 1-4.

Dramane, G., Abdoul-Azize, S., Hichami, A, Vögtle, T., Akpona, S., Chouabe, C., Sadou, H., Nieswandt, B., Besnard, P., Khan, N.A., 2012. STIM1 regulates calcium signaling in taste bud cells and preference for fat in mice. J. Clin. Invest. 122, 2267-2282.

Fatoki, O.S., Vernon, F., 1989. Determination of free fatty-acid content of polluted and unpolluted waters. Wat. Res. 23, 123-125.

343 Figueroa, V., Sáez, P.J., Salas, J.D., Salas, D., Jara, O., Martínez, A.D., Sáez, J.C.,
344 Retamal, M.A.**,** 2013. Linoleic acid induces opening of connexin26 hemichannels
345 through a PI3K/Akt/Ca^{2+}-dependent pathway. Biochim. Biophys. Acta 1828,
346 1169-1179.
347 Fink, M., Lesage, F., Duprat, F., Heurteaux, C., Reyes, R., Fosset, M., Lazdunski, M.**,**
348 1998. A neuronal two P domain K^+ channel stimulated by arachidonic acid and
349 polyunsaturated fatty acids. EMBO J. 17, 3297-3308.
350 Fukuwatari, T., Kawada, T., Tsuruta, M., Hiraoka, T., Iwanaga, T., Sugimoto, E., Fushiki,
351 T., 1997. Expression of the putative membrane fatty acid transporter (FAT) in taste
352 buds of the circumvallate papillae in rats. FEBS Lett. 414, 461-464.
353 Galindo, M.M., Voigt, N., Stein, J., van Lengerich, J., Raguse, J.D., Hofmann, T.,
354 Meyerhof, W., Behrens, M., 2012. G protein-coupled receptors in human fat taste
355 perception. Chem. Senses 37, 123-139.
356 Gilbertson, T.A., Fontenot, D.T., Liu, L., Zhang, H., Monroe, W.T., 1997. Fatty acid
357 modulation of K^+ channels in taste receptor cells: gustatory cues for dietary fat. Am. J.
358 Physiol. Cell. Physiol. 272, C1203-C1210.
359 Hamill, O.P., Marty, A., Neher, E., Sakmann, B., Sigworth, F.J., 1981. Improved
360 patch-clamp techniques for high-resolution current recording from cells and cell-free
361 membrane patches. Pflügers Arch. 391, 85-100.
362 Hoshi, T., Wissuwa, B., Tian, Y., Tajima, N., Xu, R., Bauer, M., Heinemann, S.H., Hou,
363 S., 2013. Omega-3 fatty acids lower blood pressure by directly activating
364 large-conductance Ca^{2+}-dependent K^+ channels. Proc. Natl. Acad. Sci. U S A 110,
365 4816-4821
366 Huang, Y.J., Maruyama, Y., Dvoryanchikov, G., Pereira, E., Chaudhari, N., Roper, S.D.,

2007. The role of pannexin 1 hemichannels in ATP release and cell-cell communication in mouse taste buds. Proc. Natl. Acad. Sci. U S A 104, 6436-6441.

Hwang, S.W., Cho, H., Kwak, J., Lee, S.Y., Kang, C.J., Jung, J., Cho, S., Min, K.H., Suh, Y.G., Kim, D., Oh, U., 2000. Direct activation of capsaicin receptors by products of lipoxygenases: endogenous capsaicin-like substances. Proc. Natl. Acad. Sci. USA 97, 6155-6160.

Kawai, T., Fushiki, T., 2003. Importance of lipolysis in oral cavity for orosensory detection of fat. Am. J. Physiol. Regul. Integr. Comp. Physiol. 285, R447-R454.

Laugerette, F., Passilly-Degrace, P., Patris, B., Niot, I., Febbraio, M., Montmayeur, J.P., Besnard, P., 2005. CD36 involvement in orosensory detection of dietary lipids, spontaneous fat preference, and digestive secretions. J. Clin. Invest. 115, 3177-3184.

Li, G., Sinclair, A.J., Li, D., 2011. Comparison of lipid content and fatty Acid composition in the edible meat of wild and cultured freshwater and marine fish and shrimps from china. J. Agric. Food Chem. 59, 1871-1881.

Liu, P., Shah, B.P., Croasdell, S. and Gilbertson, T.A., 2011. Transient receptor potential channel type M5 is essential for fat taste. J. Neurosci. 31, 8634-8642.

Matsumura, S., Eguchi, A., Mizushige, T., Kitabayashi, N., Tsuzuki, S., Inoue, K., Fushiki, T., 2009. Colocalization of GPR120 with phospholipase-Cβ2 and α-gustducin in the taste bud cells in mice. Neurosci. Lett. 450,186-190.

Meves, H., 2008. Arachidonic acid and ion channels: an update. Br. J. Pharmacol. 155, 4-16.

Miyamoto, T., Okada, Y, Sato, T., 1991. Voltage-gated membrane current of isolated bullfrog taste cells. Zool. Sci. 8, 835-845.

Needleman, P., Turk, J., Jakschik, B.A., Morrison, A.R., Lefkowith, J.B., 1986.

391 Arachidonic acid metabolism. Annu. Rev. Biochem. 55, 69-102.
392 Ogg, C.L., Meinke, L.J., Howard, R.W., Stanley-Samuelson, D.W., 1993. Phospholipid
393 and triacylglycerol fatty acid compositions of five species of *Diabrotica* (Insecta:
394 Coleoptera: Chrysomelidae). Comp Biochem. Physiol. 105B, 69-77.
395 Oh, D.Y., Talukdar, S., Bae, E.J., Imamura, T., Morinaga, H., Fan, W., Li, P., Lu, W.J.,
396 Watkins, S.M., Olefsky, J.M., 2010. GPR120 is an omega-3 fatty acid receptor
397 mediating potent anti-inflammatory and insulin-sensitizing effects. Cell 142,
398 687-698.
399 Okada, Y., Fujiyama, R., Miyamoto, T., Sato, T., 1996. Vasopressin modulates
400 membrane properties of taste cells isolated from bullfrogs. Chem. Senses 21,
401 739-745.
402 Okada, Y., Fujiyama, R., Miyamoto, T., Sato, T., 2001. Saccharin activates cation
403 conductance via inositol 1,4,5-trisphosphate production in a subset of isolated rod
404 taste cells in the frog. Eur. J. Neurosci. 13, 308-314.
405 Romanov, R.A., Rogachevskaja, O.A., Bystrova, M.F., Jiang, P., Margolskee, R.F.,
406 Kolesnikov, S.S., 2007. Afferent neurotransmission mediated by hemichannels in
407 mammalian taste cells. EMBO J. 26, 657-667.
408 Schmidt, D., Jiang, Q.X., MacKinnon, R., 2006. Phospholipids and the origin of
409 cationic gating charges in voltage sensors. Nature 444, 775-779.
410 Siebert, A.P., Ma, Z., Grevet, J.D., Demuro, A., Parker, I., Foskett, J.K., 2013. Structural
411 and functional similarities of calcium homeostasis modulator 1 (CALHM1) ion
412 channel with connexins, pannexins, and innexins. J. Biol. Chem. 288, 6140-6153.
413 Taruno, A., Vingtdeux, V., Ohmoto, M., Ma, Z., Dvoryanchikov, G., Li, A., Adrien, L.,
414 Zhao, H., Leung, S., Abernethy, M., Koppel, J., Davies P,, Civan, M.M., Chaudhari,

N., Matsumoto, I., Hellekant, G., Tordoff, M.G., Marambaud, P., Foskett, J.K., 2013. CALHM1 ion channel mediates purinergic neurotransmission of sweet, bitter and umami tastes. Nature 495, 223-226.

Verselis, V.K., Srinivas, M**.**, 2008. Divalent cations regulate connexin hemichannels by modulating intrinsic voltage-dependent gating. J. Gen. Physiol. 132**,** 315-327.

Watanabe, H., Vriens, J., Prenen, J., Droogmans, G., Voets, T., Nilius, B., 2003. Anandamide and arachidonic acid use epoxyeicosatrienoic acids to activate TRPV4 channels. Nature 424, 434-438.

Figure legends

Fig. 1. Effects of 50 μM arachidonic acid on the membrane properties of wing (Ib) cells in frog taste discs. The left panels (A and C) show pen recordings of the current signals at a holding potential of -54 mV. The right panels (B and D) are plots of the whole-cell current/voltage (*I/V*) relationships produced by a voltage ramp (167 mV/s) from -100 to +100 mV. The relationships labeled as a, b, and c were obtained at the times indicated by the same letters on the pen recordings. Transient outward current deflections larger than 200 pA on the pen recordings are out of scale. The pipette contained standard K^+ internal solution and the bath contained normal saline solution.

Fig. 2. Effects of internal unsaturated fatty acids on the whole-cell current/voltage (*I/V*) relationships produced by a voltage ramp (167 mV/s) from -100 to +100 mV. (A and B), time course and block with 5 mM Ba^{2+} of internal 50 μM arachidonic acid-induced currents. (C), time course and block with 5 mM Ba^{2+} of internal 50 μM eicosapentaenoic acid (ETYA)-induced current. (D), no effect of internal 50 μM linoleic acid. The pipette contained standard K^+ internal solution.

Fig. 3. Magnitudes of fatty acid-induced currents in the wing cells. (A), the pen recording of the 50 μM arachidonic acid-induced current signal at a holding potential of -55 mV. (B), plots of whole-cell current/voltage (*I/V*) relationships produced by a voltage ramp (167 mV/s) from -100 to +100 mV. The relationships labeled as a and b were obtained at the times indicated by the same letter on the pen recording and the relationship labeled as “b-a” represents the difference between a and b. (C), differences were obtained by subtracting the currents in normal saline solution from those in fatty

acid solution. Concentrations of fatty acids other than stearic acid were 50 μM. The concentration for stearic acid was 30 μM. Columns and error bars are the mean ± S.E.M. of 4-19 samples. Numerals within parentheses are the number of carbon atoms and double-bonds. The pipette contained Cs^+ internal solution and the bath contained normal saline solution.

Fig. 4. Comparison of basal, Ca^{2+}-free-induced, and linoleic acid-induced currents and conductance in wing (Ib) cells. The left panels (A, C and E) show average whole-cell current/voltage (I/V) relationships produced by a voltage ramp (167 mV/s) from -100 mV to +20 mV. Differences were obtained by subtracting basal currents in normal saline solution from those in Ca^{2+}-free saline and fatty acid solutions. The right panels (B, D, and F) show the average dependency of activation of the inward currents elicited by the voltage ramp. Conductance was calculated as $I/(V-V_{rev})$, where V_{rev} is the apparent reversal potential. The pipette contained Cs^+ internal solution.

Fig. 5. Biophysical properties of Ca^{2+}-free-induced and linoleic acid-induced currents. (A and D), the currents elicited by 400 ms voltage steps between -105 mV to +95 mV in 20 mV increments from a holding potential of -85 mV in normal saline solution. (B and E), the currents in external Ca^{2+}-free and 50 μM linoleic acid saline solutions. The initial transient inward currents were voltage-gated Na^+ currents. Leak currents were not subtracted from the current traces. (C and F), current-voltage (I/V) relationships for the currents measured at the end of the pulse in control and test conditions. Absolute current values (not differences) were plotted. The pipette contained Cs^+ internal solution.

Fig. 6. Effects of removing external Na^+ and external 100 µM flufenamic acid on linoleic acid-induced currents in wing cells. The left panels (A and C) show the pen recordings of current signals at a holding potential of -55 mV. The right panels (B and D) are plots of whole-cell current/voltage (*I/V*) relationships produced by a voltage ramp (167 mV/s) from -100 to +100 mV. The relationships labeled as a, b, and c were obtained at the times indicated by the same letters on the pen recordings. Transient outward current deflections larger than 200 pA on the pen recordings are out of scale. The pipette contained Cs^+ internal solution.

Fig. 1

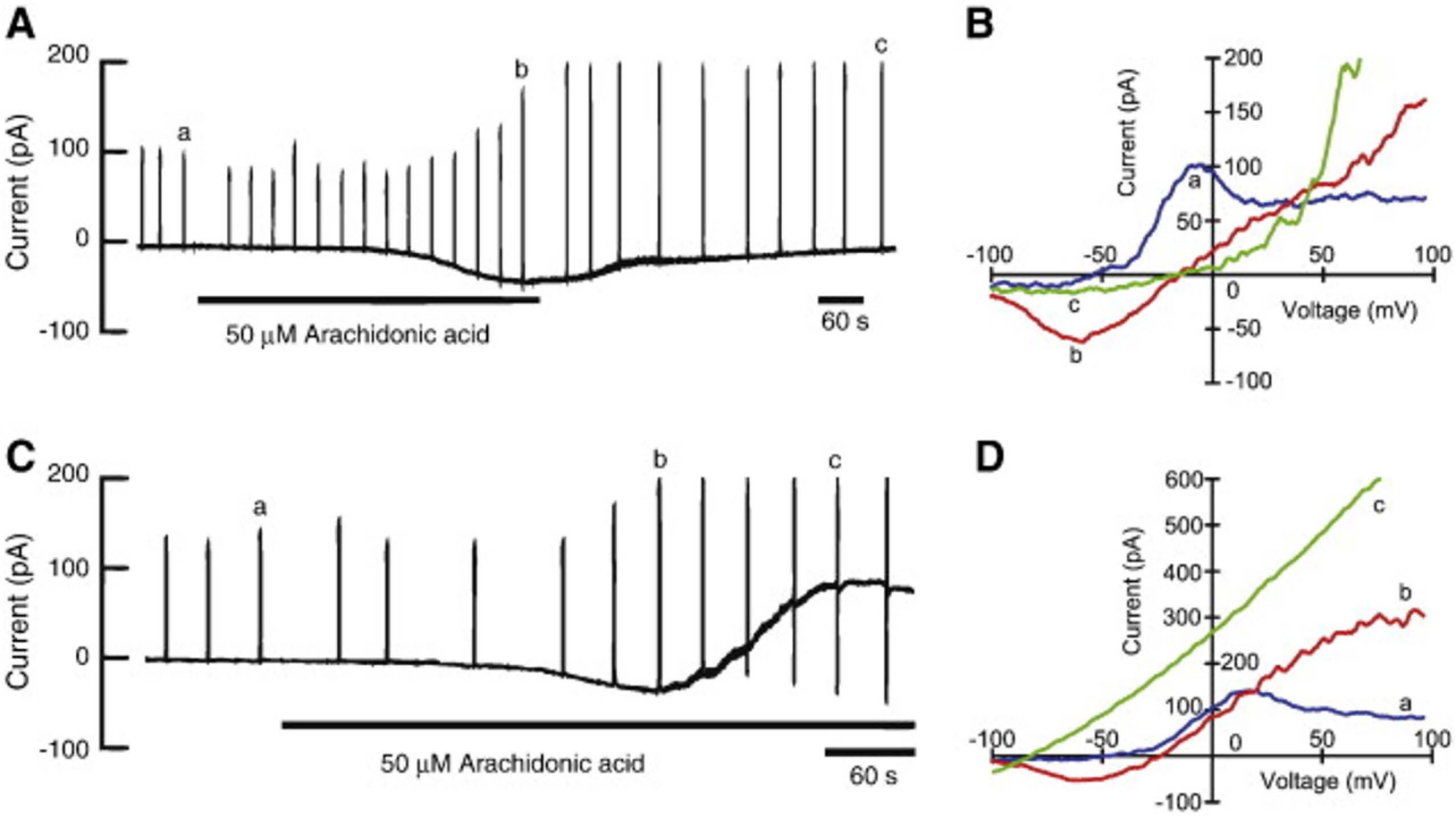
A
200
100
0
-100
Current (pA)
a
b
c
50 μM Arachidonic acid
60 s
B
200
150
100
50
0
-50
-100
-100
-50
50
100
Current (pA)
Voltage (mV)
a
b
c
C
200
100
0
-100
Current (pA)
a
b
c
50 μM Arachidonic acid
60 s
D
600
500
400
300
200
100
-100
-50
0
50
100
Current (pA)
Voltage (mV)
a
b
c

Fig. 2

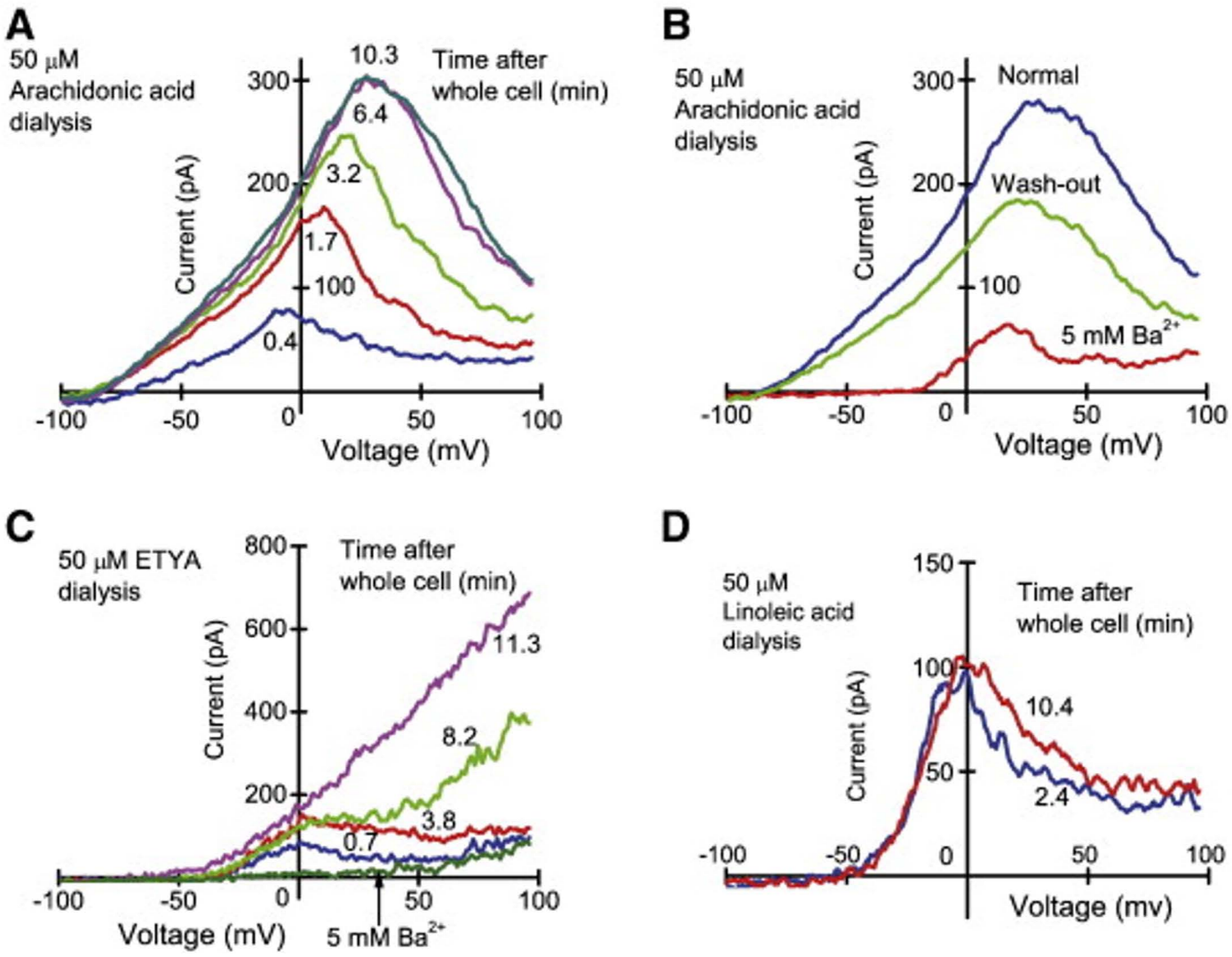
A
50 μM
Arachidonic acid
dialysis
Time after
whole cell (min)
10.3
6.4
3.2
1.7
100
0.4
Current (pA)
300
200
-100
-50
0
50
100
Voltage (mV)
B
50 μM
Arachidonic acid
dialysis
Normal
Wash-out
100
5 mM Ba2+
Current (pA)
300
200
-100
-50
0
50
100
Voltage (mV)
C
50 μM ETYA
dialysis
Time after
whole cell (min)
11.3
8.2
3.8
0.7
Current (pA)
800
600
400
200
-100
-50
0
50
100
Voltage (mV)
5 mM Ba2+
D
50 μM
Linoleic acid
dialysis
Time after
whole cell (min)
10.4
2.4
Current (pA)
150
100
50
-100
-50
0
50
100
Voltage (mv)

Fig. 3

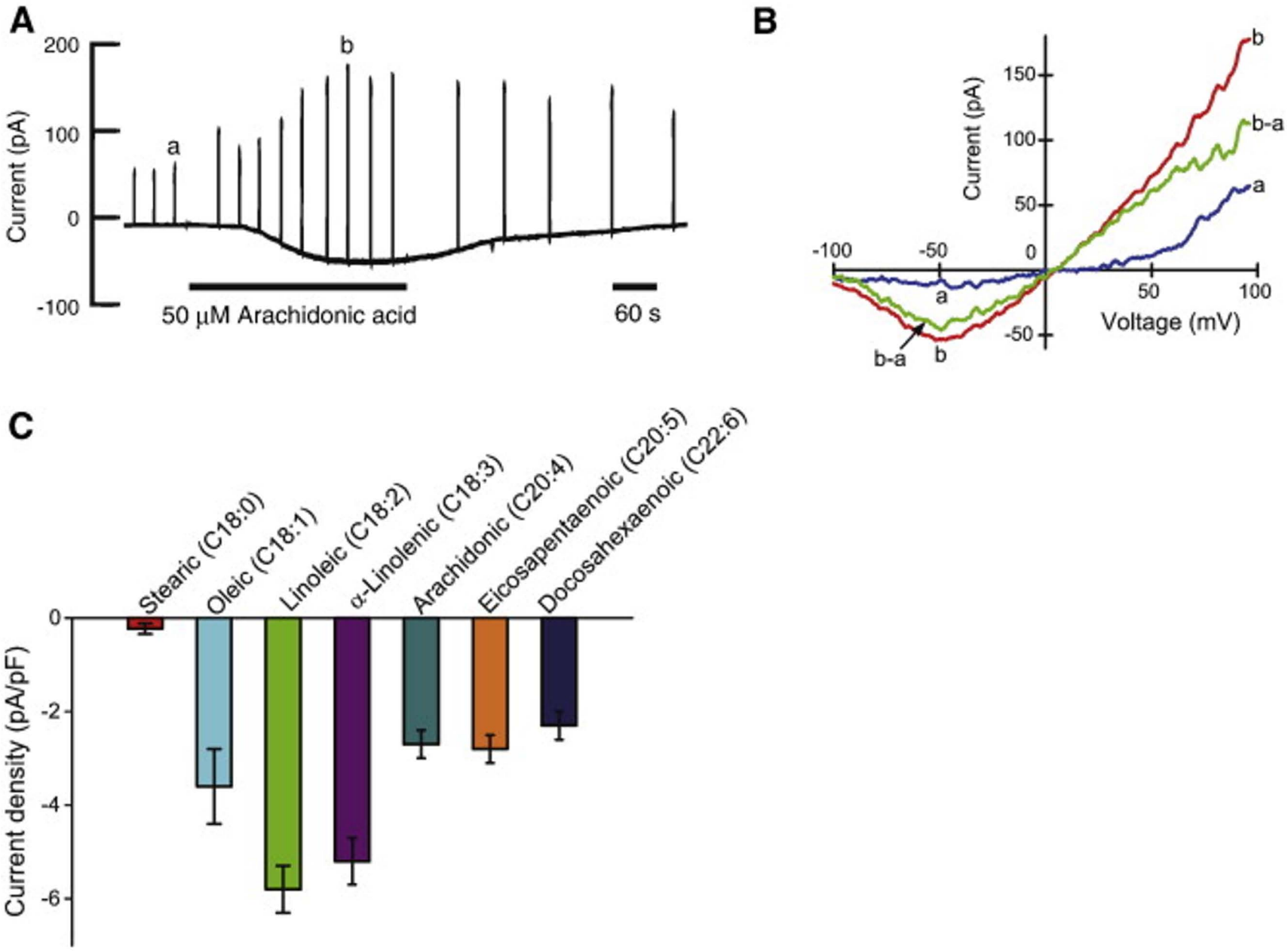
A
200
100
0
-100
Current (pA)
a
b
50 μM Arachidonic acid
60 s
B
150
100
50
-50
-100
-50
0
50
100
Current (pA)
Voltage (mV)
a
b
b-a
C
Stearic (C18:0)
Oleic (C18:1)
Linoleic (C18:2)
α-Linolenic (C18:3)
Arachidonic (C20:4)
Eicosapentaenoic (C20:5)
Docosahexaenoic (C22:6)
0
-2
-4
-6
Current density (pA/pF)

Fig. 4

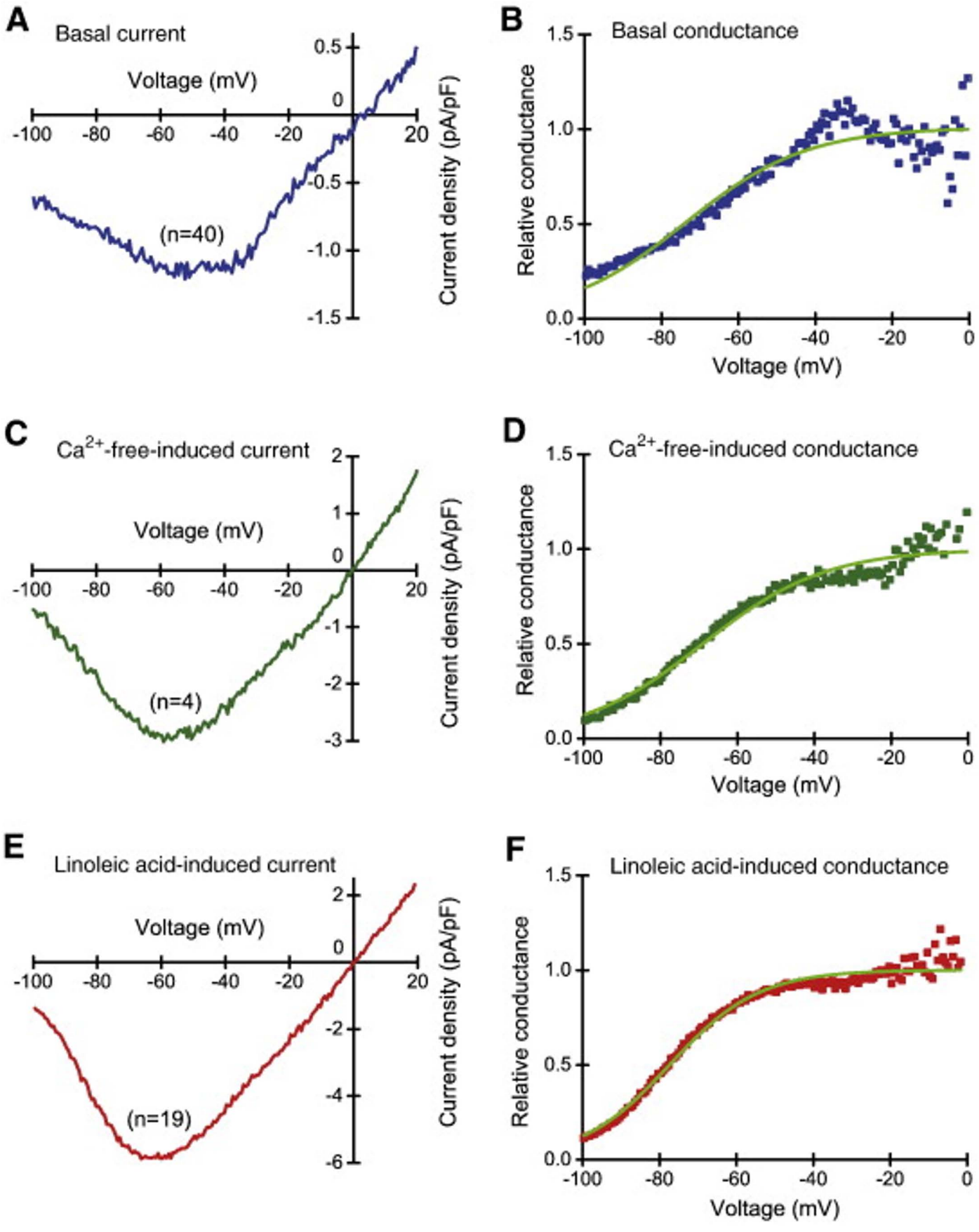
A
Basal current
Voltage (mV)
0.5
0
-100
-80
-60
-40
-20
20
-0.5
(n=40)
-1.0
-1.5
Current density (pA/pF)
B
Basal conductance
Relative conductance
1.5
1.0
0.5
0.0
-100
-80
-60
-40
-20
0
Voltage (mV)
C
Ca2+-free-induced current
Voltage (mV)
2
1
0
-100
-80
-60
-40
-20
20
-1
(n=4)
-2
-3
Current density (pA/pF)
D
Ca2+-free-induced conductance
Relative conductance
1.5
1.0
0.5
0.0
-100
-80
-60
-40
-20
0
Voltage (mV)
E
Linoleic acid-induced current
Voltage (mV)
2
0
-100
-80
-60
-40
-20
20
-2
-4
(n=19)
-6
Current density (pA/pF)
F
Linoleic acid-induced conductance
Relative conductance
1.5
1.0
0.5
0.0
-100
-80
-60
-40
-20
0
Voltage (mV)

Fig. 5

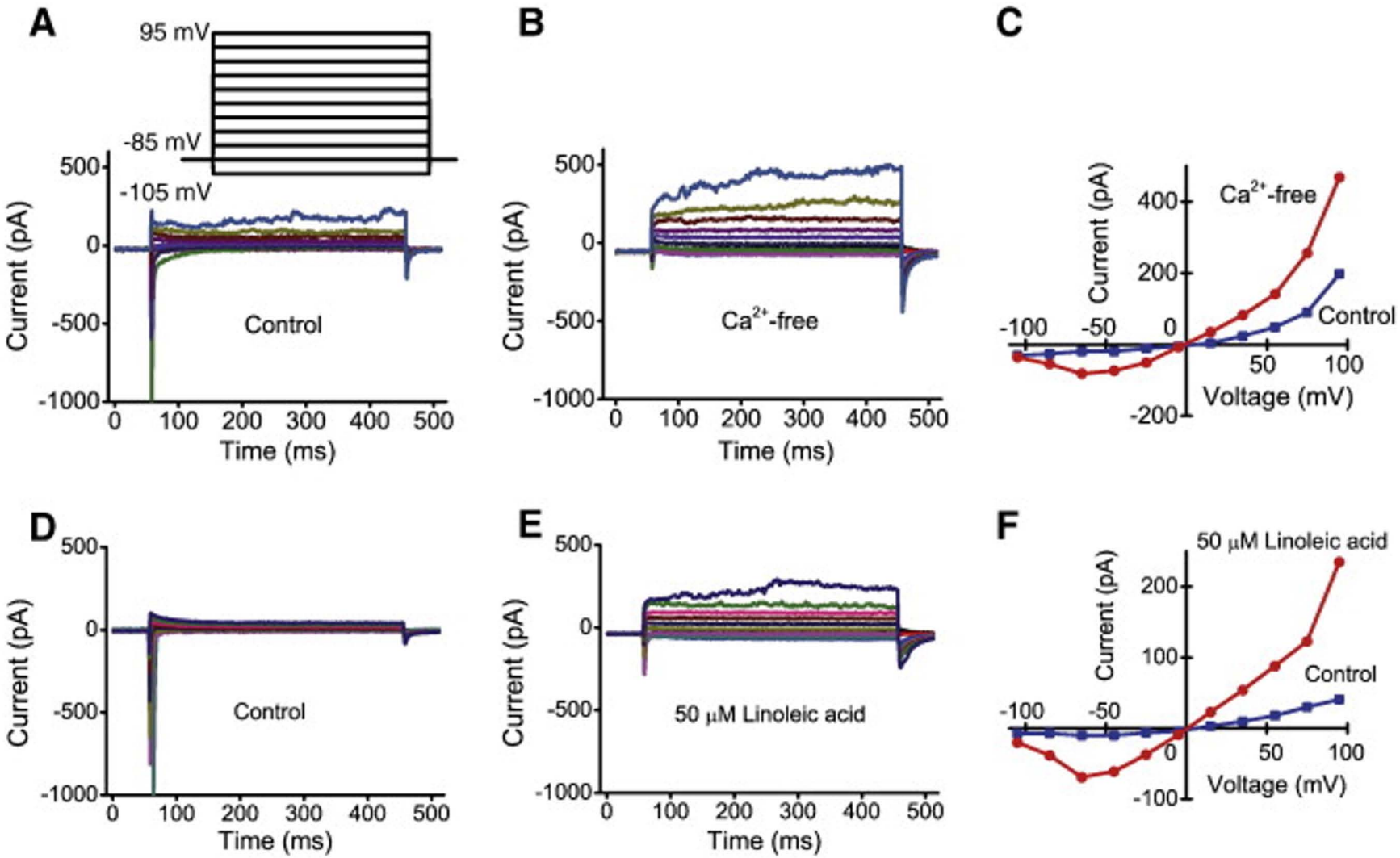
A
95 mV
-85 mV
-105 mV
Current (pA)
Time (ms)
Control
B
Ca2+-free
C
Ca2+-free
Control
Current (pA)
Voltage (mV)
D
Control
E
50 μM Linoleic acid
F
50 μM Linoleic acid
Control

Fig. 6

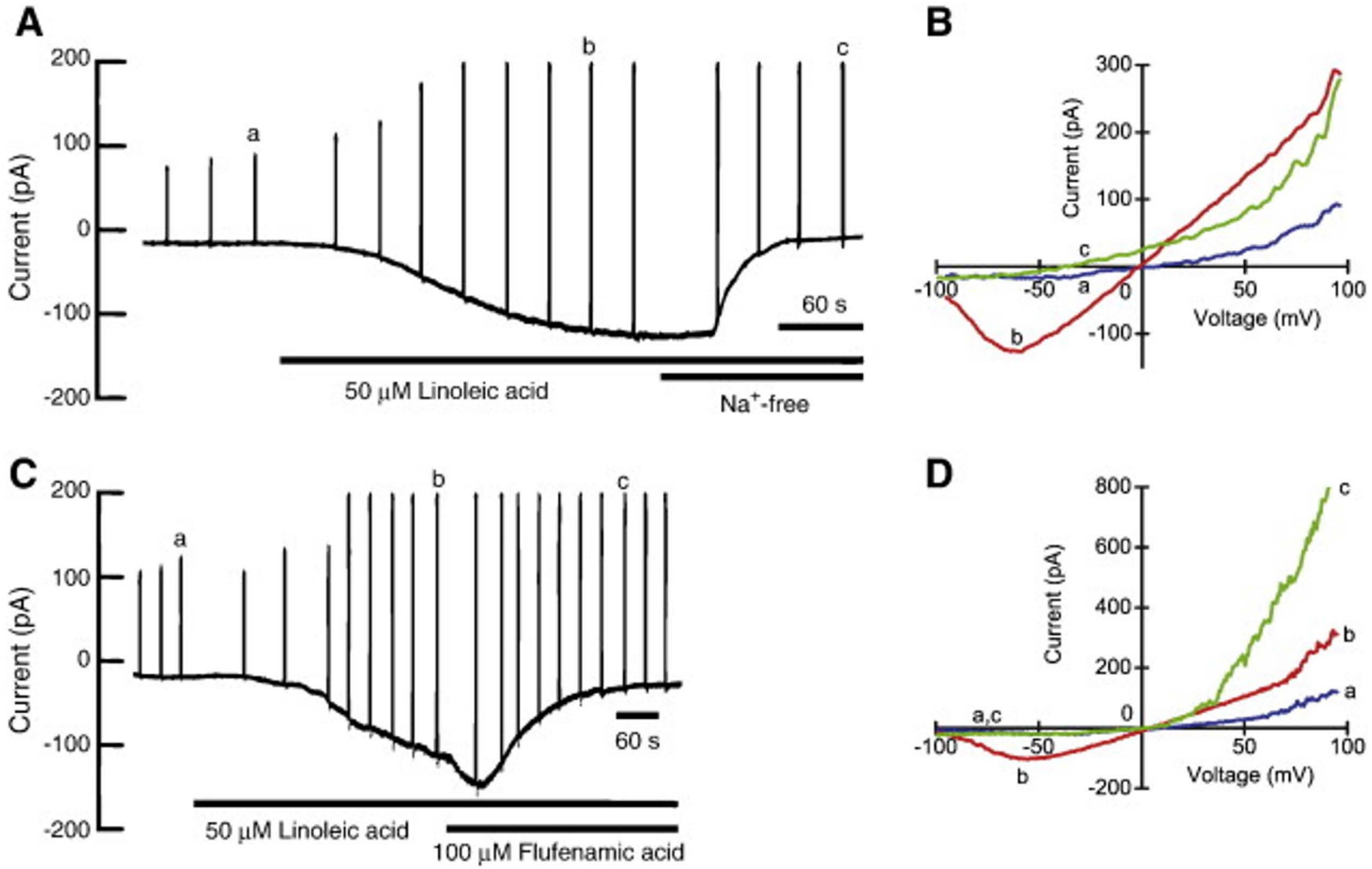
A
200
100
0
-100
-200
Current (pA)
a
b
c
60 s
50 μM Linoleic acid
Na+-free
B
300
200
100
Current (pA)
c
-100
-50
a
0
50
100
Voltage (mV)
-100
b
C
200
100
0
-100
-200
Current (pA)
a
b
c
60 s
50 μM Linoleic acid
100 μM Flufenamic acid
D
800
600
400
200
0
Current (pA)
c
b
a
a,c
-100
-50
50
100
Voltage (mV)
b
-200